Supplement of Geosci. Model Dev., 17, 4871–4890, 2024
https://doi.org/10.5194/gmd-17-4871-2024-supplement

Geoscientific Model Development
Open Access
EGU

Supplement of

Modeling biochar effects on soil organic carbon on croplands in a microbial decomposition model (MIMICS-BC_v1.0)

Mengjie Han et al.

Correspondence to: Wei Li (wli2019@tsinghua.edu.cn)

Supporting information

Table S1 Definitions, values and units of parameters in MIMICS.

Parameter	Description	Value	Unit
Carbon pools			
LIT_m	Metabolic litter pool	-	mg C cm^{-3}
LIT_S	Structural litter pool	-	mg C cm^{-3}
MIC_r	Microorganism with copiotrophic growth strategy	-	mg C cm^{-3}
MIC_k	Microorganism with oligotrophic growth strategy	-	mg C cm^{-3}
SOC_p	Physically-protected SOC pool	-	mg C cm^{-3}
SOC_c	Chemical protected SOC pool	-	mg C cm^{-3}
SOC_a	Available SOC pool	-	mg C cm^{-3}
Litter input parameters			
f_{met}	Partitioning of litter inputs to LIT_m	0.85-0.013 (lignin/N)	-
$f_{i,met}$	Fraction of litter inputs transferred to SOC_p	0.05	-
$f_{i,stru}$	Fraction of litter inputs transferred to SOC_c	0.05	-
Microbial decomposition parameters			
V_{max}	Microbial maximum reaction velocity	-	mg C (mg MIC)$^{-1}$ h^{-1}
K_m	Half-saturation constant	-	mg C cm^{-3}
V_{slope}	Regression coefficient (Eq. 2)	0.063 [a]	ln (mg C (mg MIC)$^{-1}$ h^{-1}) °C^{-1}
V_{int}	Regression intercept (Eq. 2)	5.47 [a]	ln (mg C (mg MIC)$^{-1}$ h^{-1})
av	Tuning coefficient (Eq. 2)	8×10^{-6} [a]	-
V_{mod-r}	Modifies V_{max} for fluxes into MIC_r	10, 2, 10 [b]	-
V_{mod-k}	Modifies V_{max} for fluxes into MIC_k	3,3,2 [c]	-
K_{slope}	Regression coefficient (Eq. 3)	0.017, 0.027, 0.017 [b, c]	ln (mg C cm^{-3}) °C^{-1}
K_{int}	Regression intercept (Eq. 3)	3.19 [a]	ln (mg C cm^{-3})
ak	Tuning coefficient (Eq. 3)	10 [a]	-
K_{mod-r}	Modifies K_m for fluxes into MIC_r	0.125,0.5,0.25×P_{scalar} [b]	-
K_{mod-k}	Modifies K_m for fluxes into MIC_k	0.5,0.25,0.167×P_{scalar} [c]	-
P_{scalar}	Physical protection scalar used in K_{mod}	$(2.0 \times (2.0 \times e^{-2\sqrt{fclay}})^{-1}$	-
MGE	Microbial growth efficiency	0.5,0.25,0.7,0.35 [d]	mg mg^{-1}
k_{mic}	Microbial biomass turnover rate	$5.2 \times 10^{-4} \times e^{0.3(fmet)} \times \tau_{mod}$ [e]	h^{-1}
		$2.4 \times 10^{-4} \times e^{0.1(fmet)} \times \tau_{mod}$ [e]	
τ_{mod}	Modifies microbial turnover rate	$0.8 < \sqrt{NPP/100} < 1.2$	-
a_τ	Tuning coefficient of K_{mic}	1.0	-
f_{rp}	Fraction of K_{mic} of MIC_r partitioned to SOC_p	$min\ (1.0, 0.13 \times e^{1.3(fclay)})$ [f]	-
f_{kp}	Fraction of K_{mic} of MIC_k partitioned to SOC_p	$min\ (1.0, 0.02 \times e^{0.8(fclay)})$ [f]	
f_{rc}	Fraction of K_{mic} of MIC_r partitioned to SOC_c	$min\ (1.0 - f_{rp}, 1.06 \times e^{-2.6(fmet)})$ [f]	-
f_{kc}	Fraction of K_{mic} of MIC_k partitioned to SOC_c	$min\ (1.0 - f_{kp}, 8.93 \times e^{-2.6(fmet)})$ [f]	
f_{ra}	Fraction of K_{mic} of MIC_r partitioned to SOC_a	$1.0 - f_{rp} - f_{rc}$	-
f_{ka}	Fraction of K_{mic} of MIC_k partitioned to SOC_a	$1.0 - f_{kp} - f_{kc}$	
β	Density-dependence exponent	Eq. 6	-
Protected carbon parameters			
D	Desorption rate from SOC_p to SOC_a	Eq. 5	h^{-1}
KO	Further modifies K_m for oxidation of SOC_c	4, 4 [e]	-

Parameter	Description	Value	Unit
k_d	Tuning coefficient of the desorption rate	Eq. 5	-
K_{ads}	The sorption rate of SOC_p	Eq. 8	h^{-1}
k_{ba}	The binding affinity (Eq. 8)	1~16 [g]	$(mg\ C \cdot mg^{-3})^{-1}$
Q_{max}	The maximum sorption capacity of SOC_p	Eq. 9	$mg\ C\ cm^{-3}$
Biochar-related parameters			
f_{bp}	Fraction of biochar carbon partitioned into SOC_p	0.6	-
f_{ba}	Fraction of biochar carbon partitioned into SOC_a	0.03-0.3 [h]	-
f_{bc}	Fraction of biochar carbon partitioned into SOC_c	$1.0 - f_{bp} - f_{ba}$	-
f_{loss}	Biochar fraction loss during addition	0.02 [h]	-
f_d	Coefficients for adjusting the desorption rate of SOC_p with biochar addition (Eq. 15)	-0.15 ~0.15 [h]	$ha\ t^{-1}\ C$
f_v	Coefficients for adjusting the microbial decomposition velocity with biochar addition (Eq. 16)	-0.15 ~0.15 [h]	$ha\ t^{-1}\ C$

[a] From observations in German et al. (2012), as used in Wieder et al. (2014, 2015).

[b] For LIT_m, LIT_s, and SOC_a, fluxes entering MIC_r, respectively.

[c] For LIT_m, LIT_s, and SOC_a, fluxes entering MIC_k, respectively.

[d] 0.5 is the MGE of C fluxes from LIT_m and SOC_a to MIC_r, 0.25 is for C flux from LIT_s to MIC_r, 0.7 is for fluxes from LIT_s and SOC_a to MIC_k, 0.35 is for C flux from LIT_m to MIC_k.

[e] For MIC_r and MIC_k, respectively.

[f] Values from Zhang et al. (2020).

[g] Values from Wang et al. (2020).

[h] Ranges from Archontoulis et al. (2016).

Table S2 Definitions and values of modified parameters used in default MIMICS.

Parameters[d]	Description	Original values[a]	Modified values
cn_leaf	The ratio of carbon to nitrogen in leaf	30	25[b]
cn_root	The ratio of carbon to nitrogen in root	75	45[b]
cn_stem	The ratio of carbon to nitrogen in stem	200	50[b]
lig_c_leaf	The ratio of lignin to carbon in leaf	0.1	0.12[b]
lig_c_root	The ratio of lignin to carbon in root	0.1	0.40[b]
lig_c_stem	The ratio of lignin to carbon in stem	0.15	0.15[b]
HI	Harvest index	-	0.45[c]

[a] Values based on Zhang et al. (2020).

[b] Estimated values from Abiven et al. (2005).

[c] Value from Hicke and Lobell (2004).

[d] These parameters were assumed unchanged with biochar addition.

Table S3 Prior parameter values, optimized values and ranges in the parameter optimization for various MIMICS versions.

Datasets	Model	Parameter	Prior value	Optimized value	Range[c]	Units
MIMICS	MIMICS-def	a_v	10	13.95	[0,30]	-
		a_k	5	16.36	[0,20]	-
		k_d	0.5	1.73	[0,3]	-
	MIMICS-T	a_v	10	8.34	[0,30]	-
		a_k	5	12.52	[0,20]	-
		k_d	0.5	2.57	[0,3]	-
		β	1	1.15	[0,2]	-
	MIMICS-TS	a_v	10	9.13	[0,30]	-
		a_k	5	17.72	[0,20]	-
		k_d	0.5	2.15	[0,3]	-
		β	1	1.35	[0,2]	-
		k_{ba}	6	8.60	[1,16]	-
		c_1	0.3	0.27	[0,0.8]	-
		c_2	3.0	2.16	[0,5]	-
	MIMICS-TSM_a	a_v	10	8.50	[0,30]	-
		a_k	5	15.22	[0,20]	-
		k_d	0.5	2.03	[0,3]	-
		β	1	1.33	[0,2]	-
		k_{ba}	6	8.38	[1,16]	-
		c_1	0.3	0.42	[0,0.8]	-
		c_2	3	2.61	[0,5]	-
	MIMICS-TSM_b	a_v	10	9.94	[0,30]	-
		a_k	5	19.42	[0,20]	-
		k_d	0.5	1.97	[0,3]	-
		β	1	1.36	[0,2]	-
		k_{ba}	6	6.51	[1,16]	-
		c_1	0.3	0.39	[0,0.8]	-
		c_2	3	1.55	[0,5]	-
	MIMICS-TSM_c	a_v	10	10.37	[0,30]	-
		a_k	5	17.12	[0,20]	-
		k_d	0.5	1.63	[0,3]	-
		β	1	1.21	[0,2]	-
		k_{ba}	6	9.61	[1,16]	-
		c_1	0.3	0.28	[0,0.8]	-
		c_2	3	2.24	[0,5]	-
$MIMICS_T$-BC	$MIMICS_T$-BC_{def}	none	none	none	none	none
	$MIMICS_T$-BC_D	f_d	-0.002	-0.0084[a] (-0.0131[b])	[-0.15,0.15]	ha t^{-1} C
	$MIMICS_T$-BC_{DV}	f_d	-0.002	0.0168[a] (-0.0125[b])	[-0.15,0.15]	ha t^{-1} C
		f_v	0.05	-0.0086[a] (-0.0149[b])	[-0.15,0.15]	ha t^{-1} C
	$MIMICS_T$-$BC_{DV\text{-}SOCa}$	f_d	-0.002	-0.0096[a] (-0.0030[b])	[-0.15,0.15]	ha t^{-1} C

		f_v	0.05	0.0082[a] (-0.0257[b])	[-0.15,0.15]	ha t^{-1} C
$MIMICS_{TSMb}$-BC	$MIMICS_{TSMb}$-BC_{def}	none	none	none	none	none
	$MIMICS_{TSMb}$-BC_{D}	f_d	-0.002	-0.0121[a] (-0.0122[b])	[-0.15,0.15]	ha t^{-1} C
	$MIMICS_{TSMb}$-BC_{DV}	f_d	-0.002	0.0020 [a] (0.0934[b])	[-0.15,0.15]	ha t^{-1} C
		f_v	0.05	-0.0092 [a] (-0.0253[b])	[-0.15,0.15]	ha t^{-1} C
	$MIMICS_{TSMb}$-$BC_{DV\text{-}SOCa}$	f_d	-0.002	0.0020[a] (0.0107[b])	[-0.15,0.15]	ha t^{-1} C
		f_v	0.05	-0.0098[a] (-0.0260[b])	[-0.15,0.15]	ha t^{-1} C

[a] The optimized parameter values using the short-term SOC data.

[b] The optimized parameter values using the long-term (extended to 8 yr) SOC data.

[c] The prescribed parameter ranges of a_v, a_k, k_d, β are from Zhang et al. (2020). k_{ba} is from Wang et al. (2020). c_1 and c_2 are estimated from Mayes et al. (2012). f_d and f_v are from Archontoulis et al. (2016).

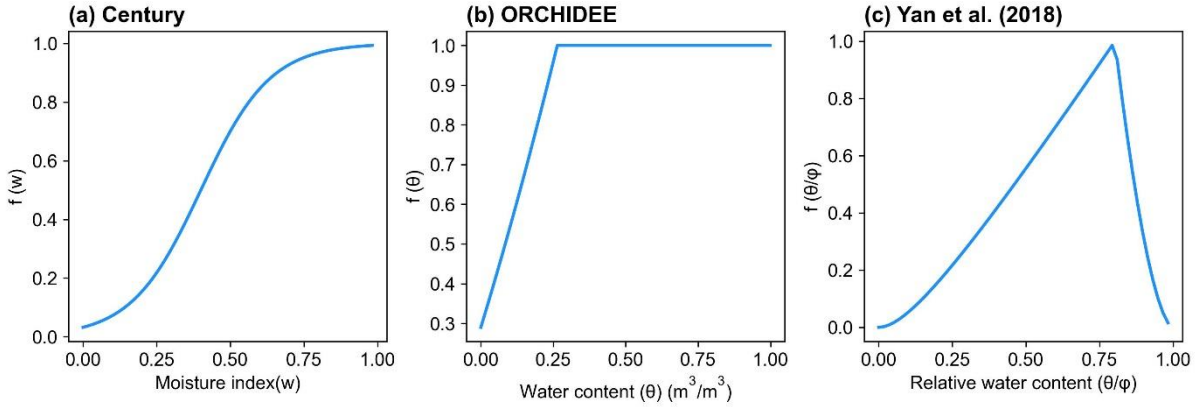

Fig. S1 Soil moisture functions from (a) the Century model (Parton et al., 2000), (b) the ORCHIDEE-SOM model (Camino-Serrano et al., 2018) and (c) the mechanism-based soil moisture function from Yan et al. (2018). *w* is soil moisture indicator (AI, i.e., precipitation/potential evapotranspiration). θ is soil water content, φ is soil porosity, and θ/φ is relative water content.

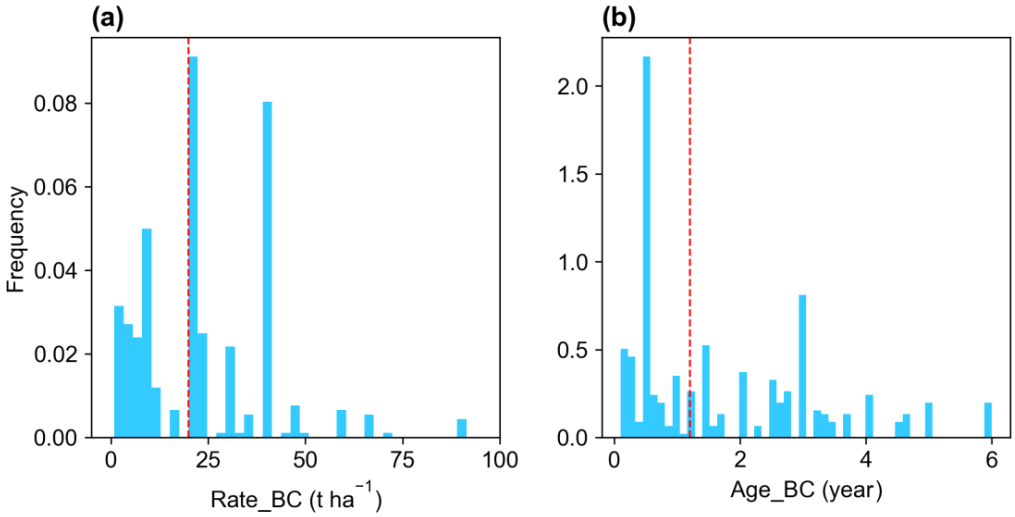

Fig. S2 The frequency distribution of (a) biochar application rates (Rate_BC) and (b) biochar addition periods (Age_BC). Red dotted lines indicate the median values.

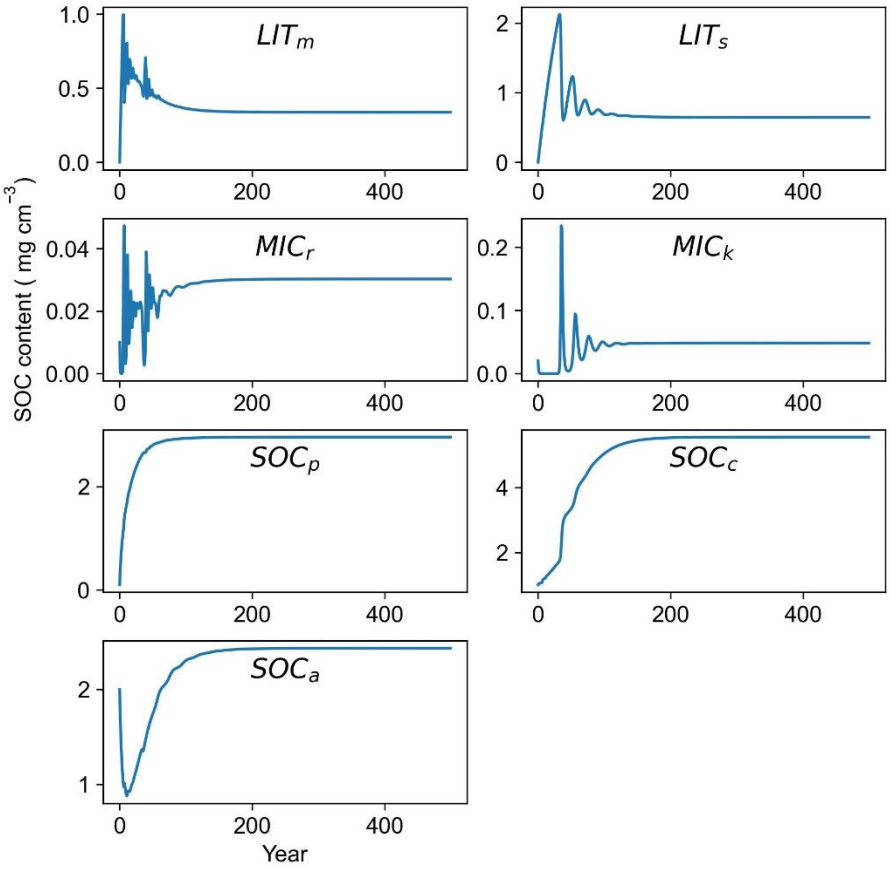

Fig. S3 Temporal changes of seven SOC pools from a simulation of the MIMICS-TSM$_b$ version for 500 years using one random site (Lat, Lon =28.1°N, 113.2°E) as an example.

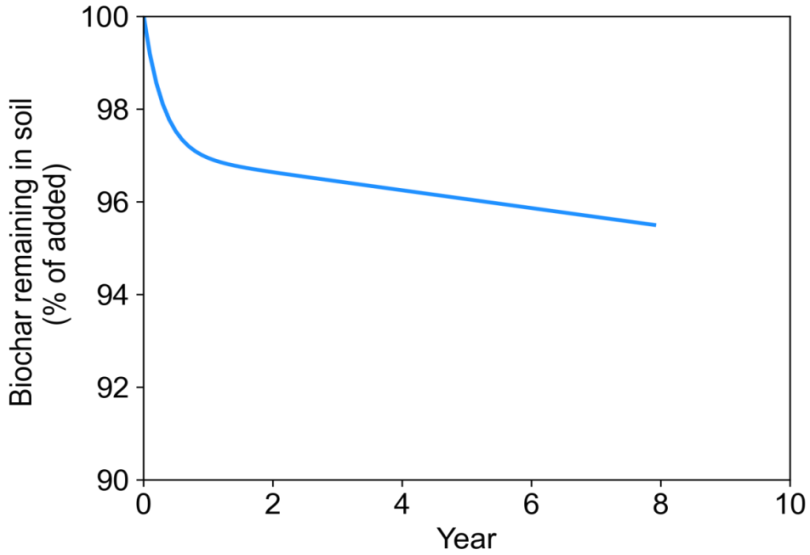

Fig. S4 The biochar decomposition curve fitted with experimental data from Wang et al. (2016) using a double first-order exponential decay model ($BC_{remain\%} = 3.02 \times e^{(-3.24 \times age\_bc)} + 97.02 \times e^{(-0.002 \times age\_bc)}$).

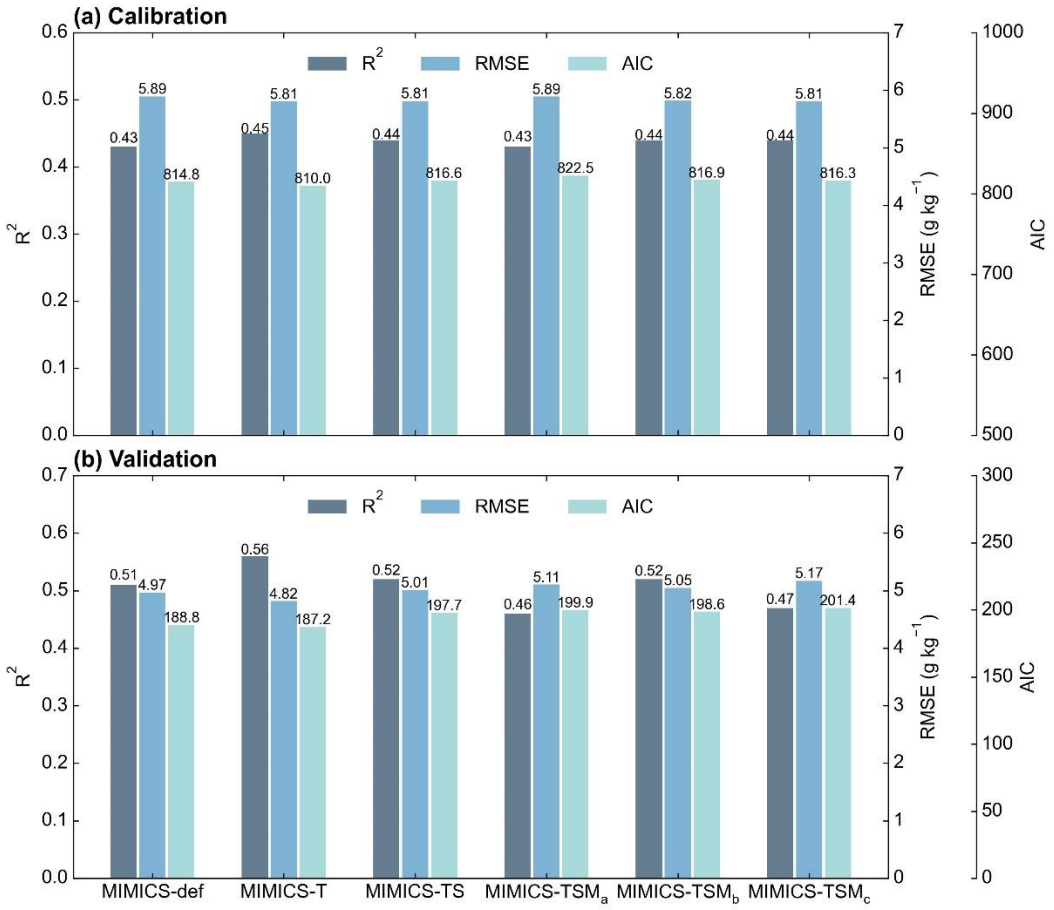

Fig. S5 Comparison of R^2, RMSE and AIC of all MIMICS versions in model calibration (a) and validation (b).

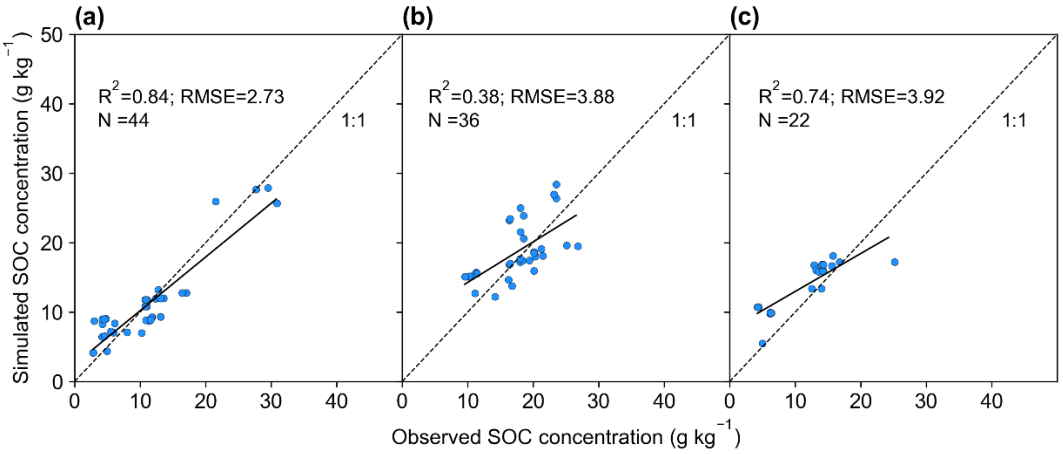

Fig. S6 Relationship between observed and simulated SOC concentrations by MIMICS-TSM$_b$ for (a) maize, (b) rice and (c) wheat. The unit of RMSE is g kg^{-1}.

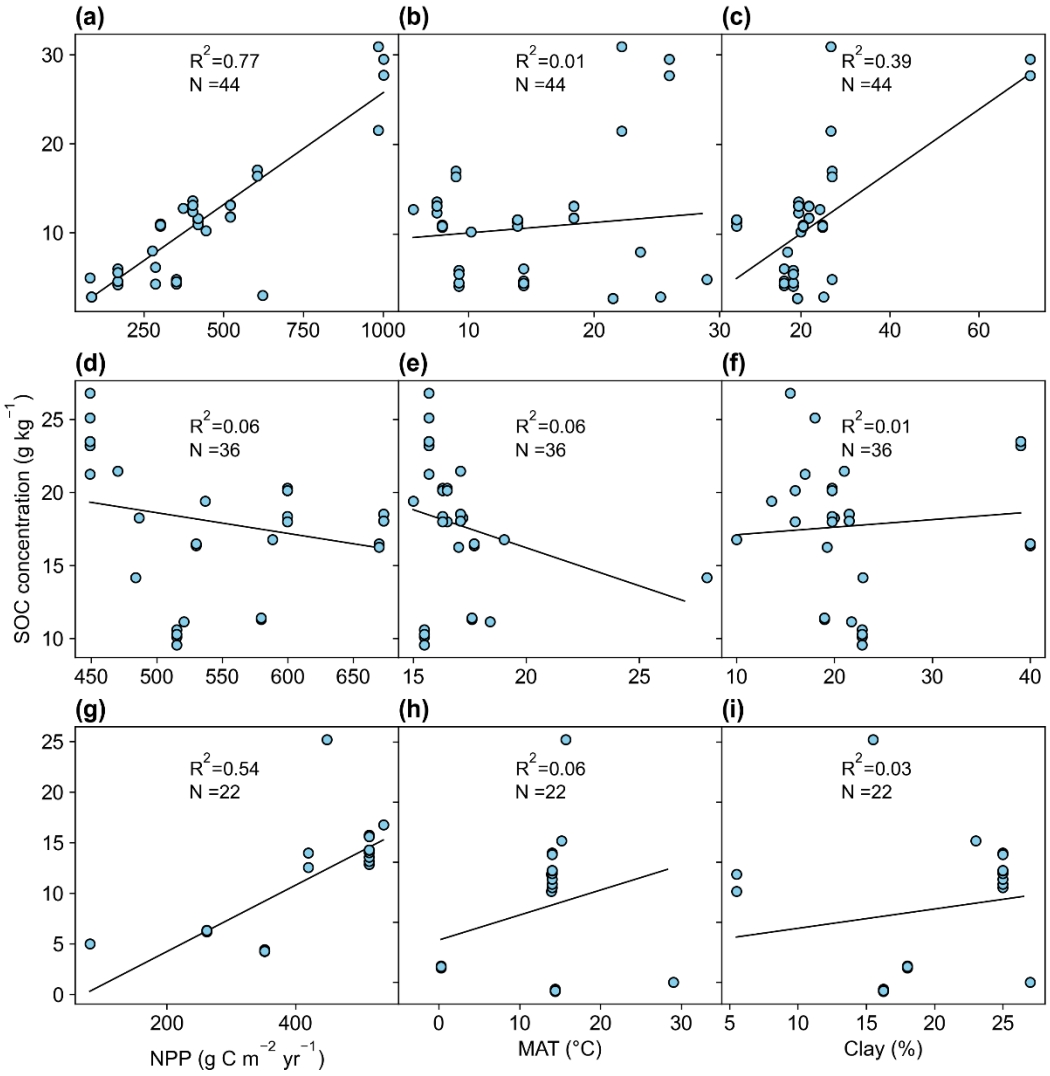

Fig. S7 Correlation between SOC concentrations with NPP, MAT and Clay for maize (a-c), rice (d-f) and wheat (g-i).

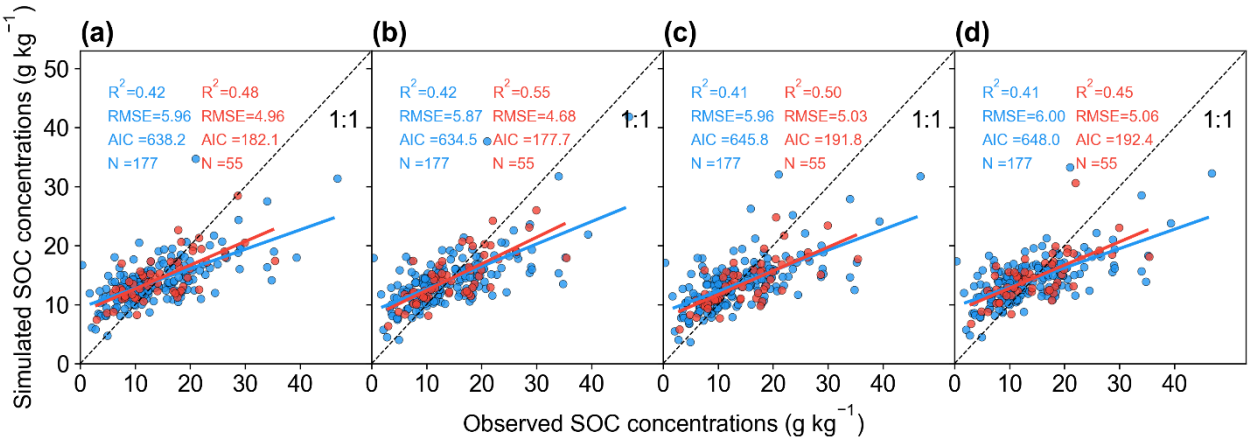

Fig. S8 Relationships between observed and simulated SOC concentrations aggregated within each 0.5° grid cell by MIMICS-def (a), MIMICS-T (b), MIMICS-TS (c) and MIMICS-TSM$_b$ (d). The unit of RMSE is g kg^{-1}. Blue and red dots represent observation sites for model calibration (80% sites) and validation (20% sites), respectively.

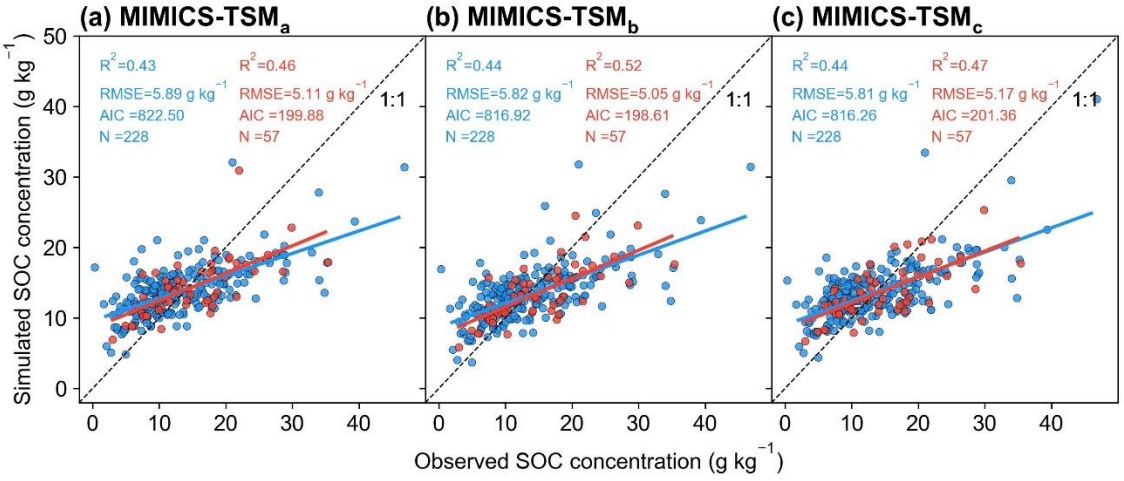

Fig. S9 Comparison between the observed and simulated SOC concentrations by (a) MIMICS-TSM$_a$, (b) MIMICS-TSM$_b$ and (c) MIMICS-TSM$_c$. Blue and red dots represent observation sites for model calibration (80% sites) and validation (20% sites), respectively.

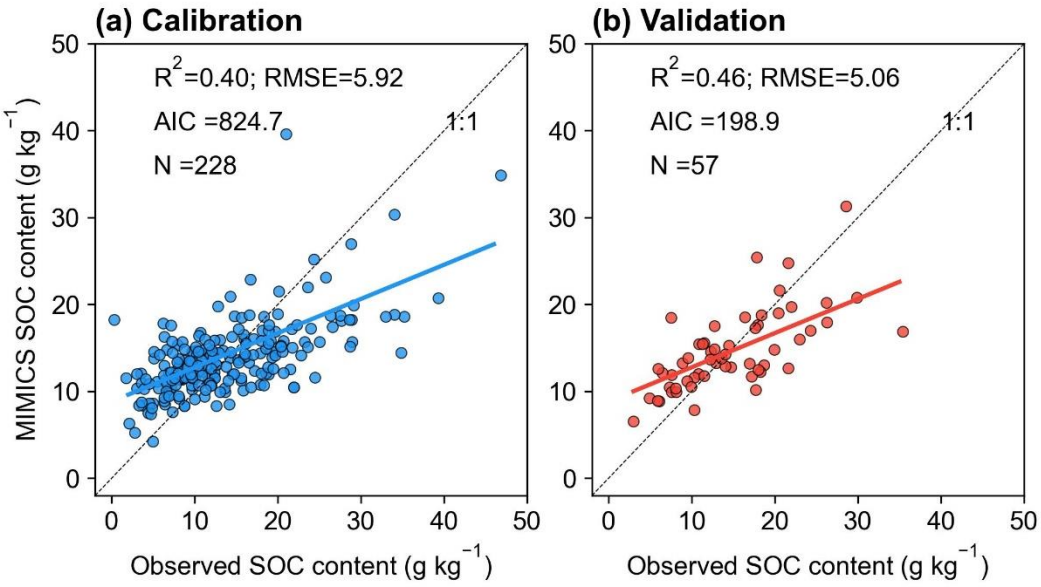

105

Fig. S10 Relationships between observed and simulated SOC concentrations by MIMICS-TSM$_b$ for (a) calibration and (b) validation assuming that the soil moist factor ($f_{m2}(\theta)$, Eq. 11) were multiplied by V_{max} and microbial turnover (τ) of MIC_r and MIC_k, instead of by V_{max} and K_m in **Section 2.1.4**.

110

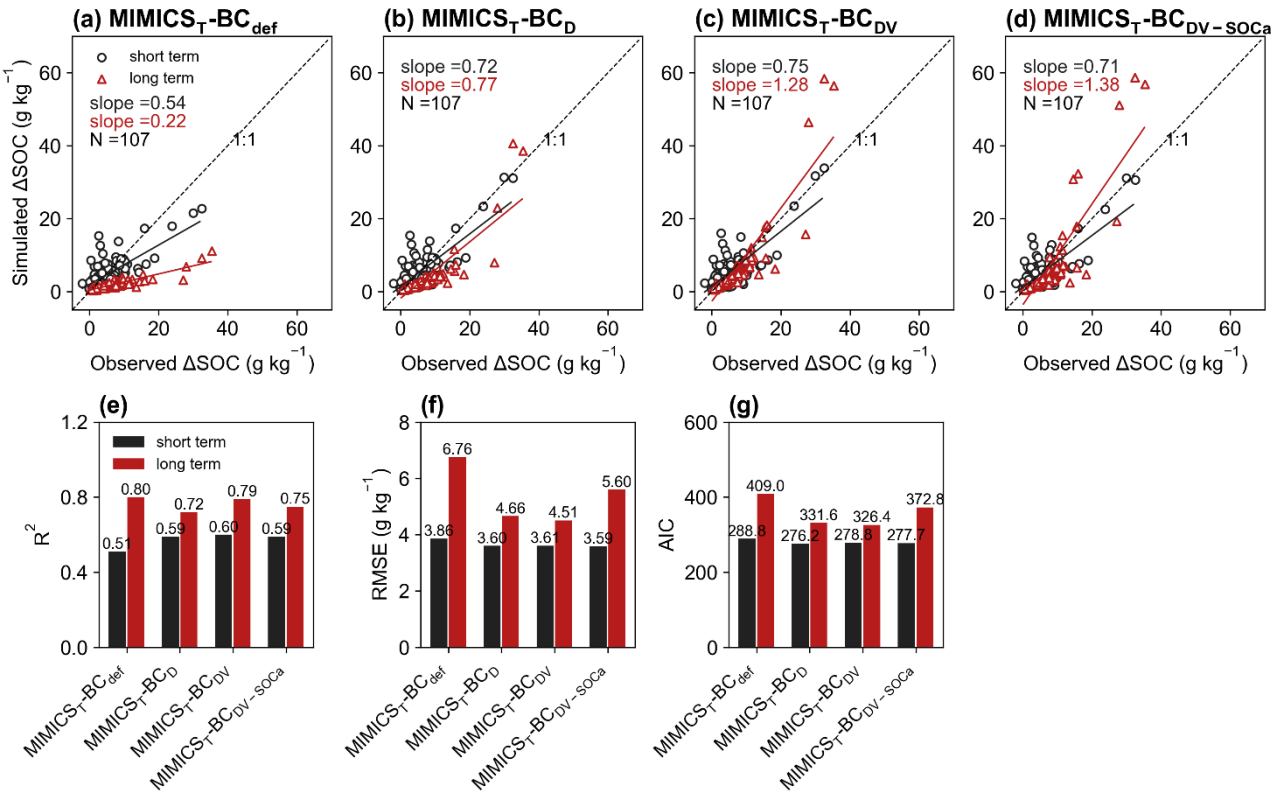

Fig. S11 As Fig. 6 but for model calibration instead of validation.

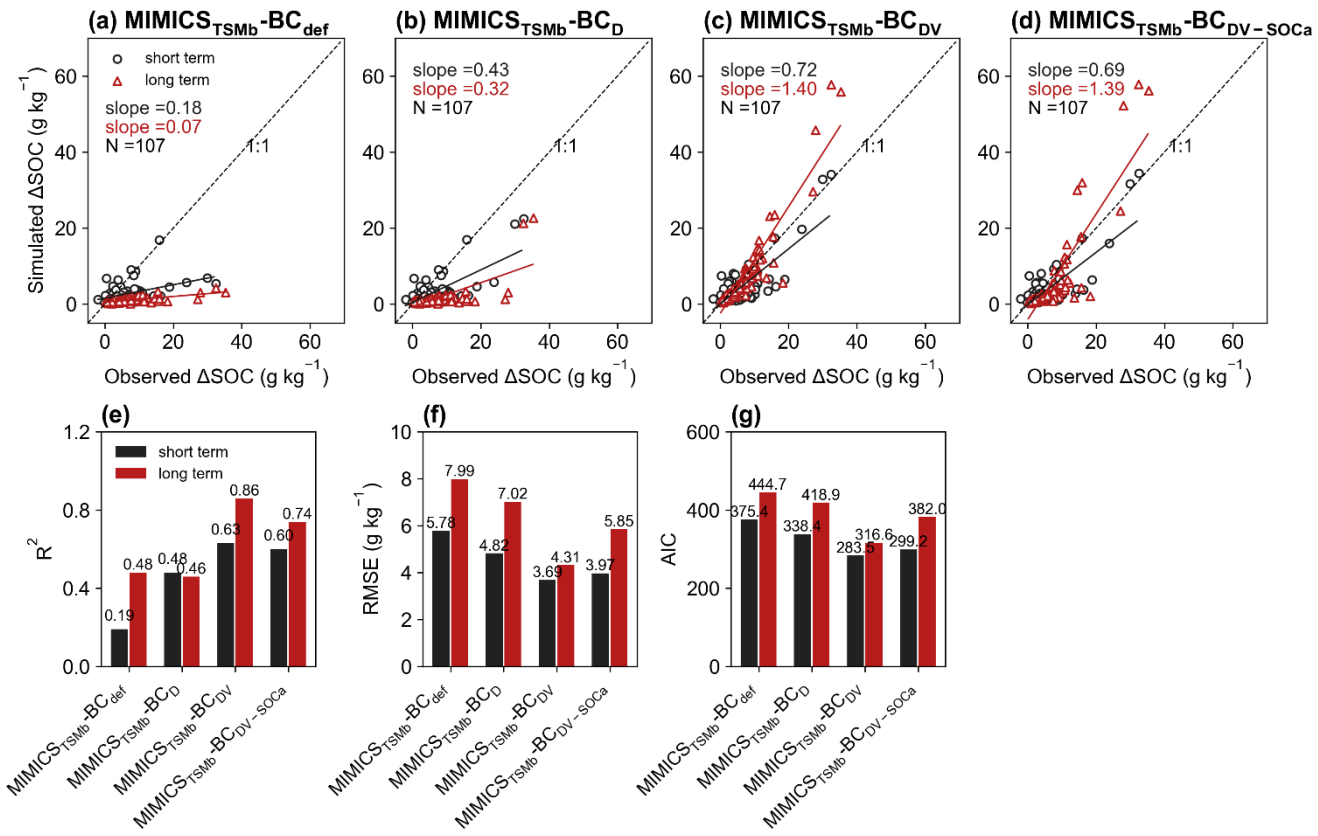

115 **Fig. S12** As Fig. 7 but for model calibration instead of validation.

120

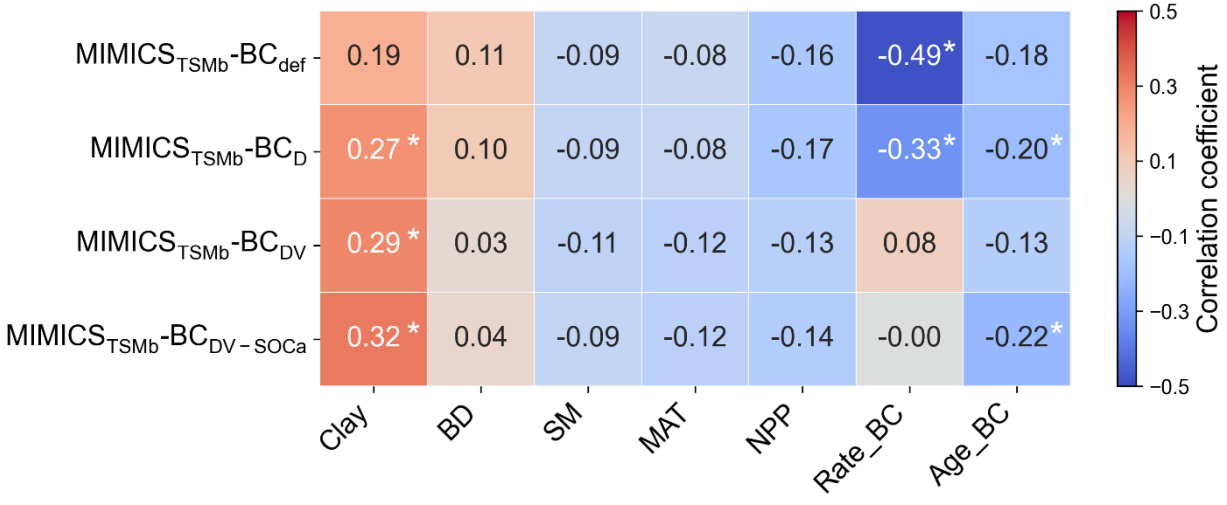

Fig. S13 As Fig. 8 but for short-term SOC changes with biochar addition.

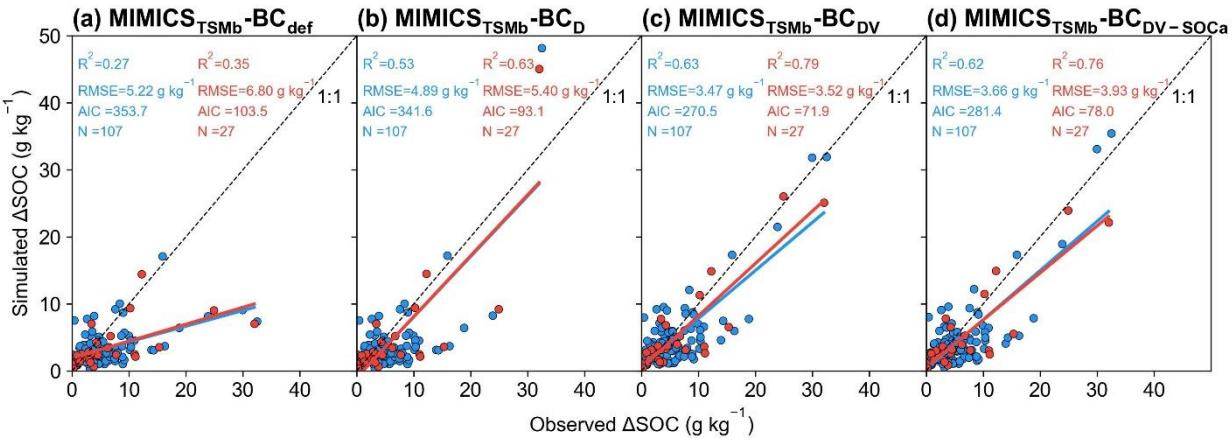

125

Fig. S14 Relationships of short-term SOC changes after biochar addition between observations and models with (a) MIMICS$_{TSMb}$-BC$_{def}$, (b) MIMICS$_{TSMb}$-BC$_{D}$, (c) MIMICS$_{TSMb}$-BC$_{DV}$ and (d) MIMICS$_{TSMb}$-BC$_{DV-SOCa}$. (f_{ba}=2%). Blue and red dots represent observation sites for model calibration (80% sites) and validation (20% sites), respectively.

130

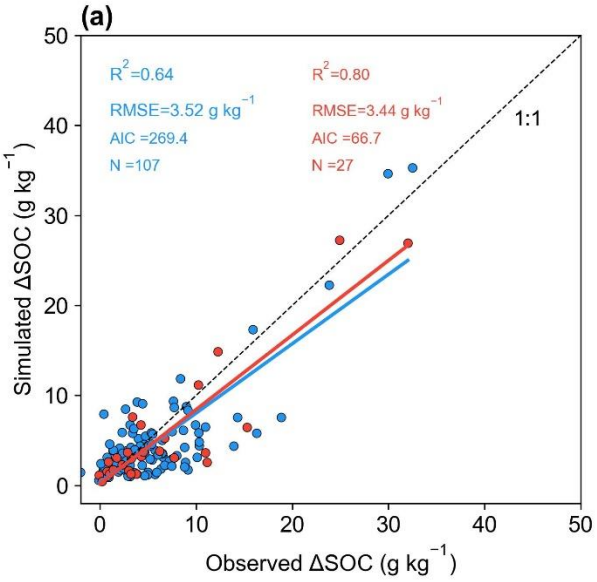

135

Fig. S15 Relationships of short-term SOC changes after biochar addition between observations and models simulated with MIMICS$_{TSMb}$-BC$_{DV}$ version with four parameters optimized (optimized values: f_d=0.1123, f_v=-0.0088, f_{bp}=0.581 and f_{ba}=0.0816). Blue and red dots represent observation sites for model calibration (80% sites) and validation (20% sites), respectively.

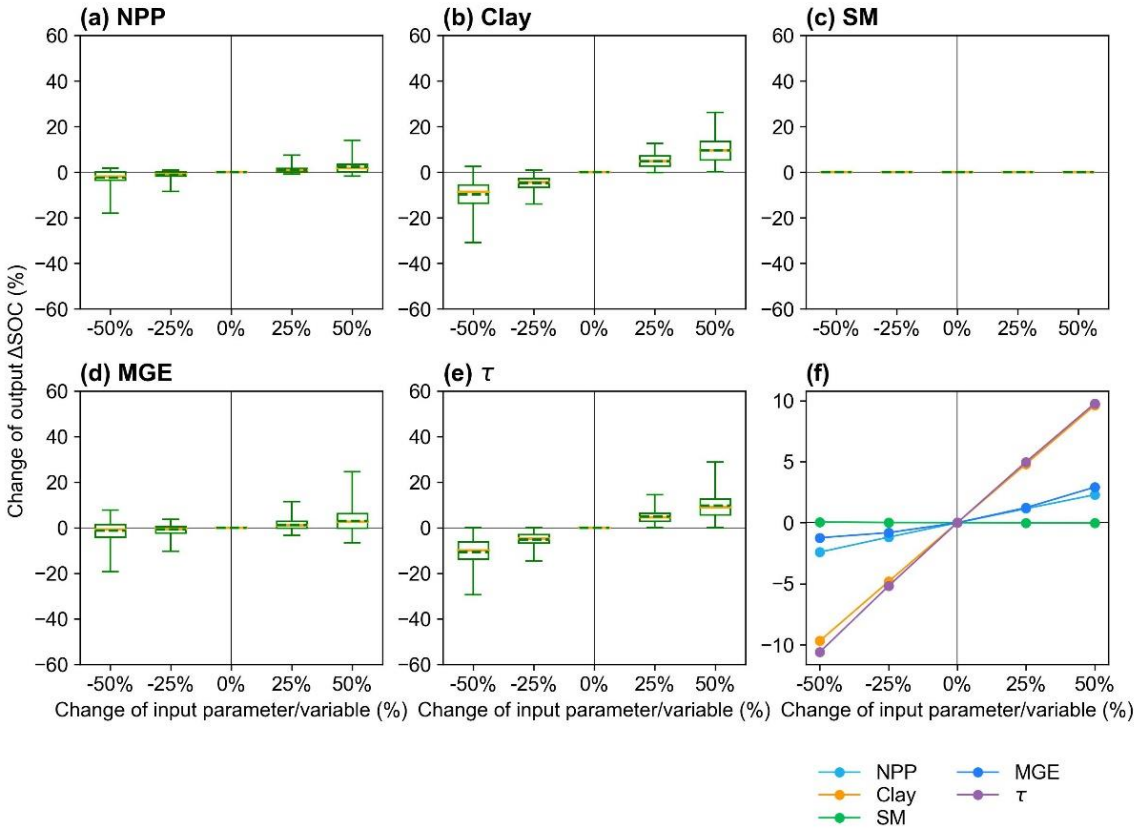

Fig. S16 Sensitivity analysis of MIMICS$_{TSMb}$-BC$_{DV}$ model input variables of (a) NPP, (b) Clay, (c) SM and parameters of (d) MGE (microbial growth efficiency, Fig. 1) and (e) τ (microbial biomass turnover, Fig. 1). The yellow line and green dotted line in boxplot are median and mean values of output variable change (i.e., change of ΔSOC, Eq. 19). The means of ΔSOC changes with perturbations in calibrated sites are plot in (f).

References

Abiven, S., Recous, S., Reyes, V., and Oliver, R.: Mineralisation of C and N from root, stem and leaf residues in soil and role of their biochemical quality, Biology and Fertility of Soils, 42, 119-128, 10.1007/s00374-005-0006-0, 2005.

Archontoulis, S. V., Huber, I., Miguez, F. E., Thorburn, P. J., Rogovska, N., and Laird, D. A.: A model for mechanistic and system assessments of biochar effects on soils and crops and trade‐offs, GCB Bioenergy, 8, 1028-1045, 10.1111/gcbb.12314, 2016.

Camino-Serrano, M., Guenet, B., Luyssaert, S., Ciais, P., Bastrikov, V., De Vos, B., Gielen, B., Gleixner, G., Jornet-Puig, A., Kaiser, K., Kothawala, D., Lauerwald, R., Peñuelas, J., Schrumpf, M., Vicca, S., Vuichard, N., Walmsley, D., and Janssens, I. A.: ORCHIDEE-SOM: modeling soil organic carbon (SOC) and dissolved organic carbon (DOC) dynamics along vertical soil profiles in Europe, Geoscientific Model Development, 11, 937-957, 10.5194/gmd-11-937-2018, 2018.

German, D. P., Marcelo, K. R., Stone, M. M., and Allison, S. D.: The Michaelis‐Menten kinetics of soil extracellular enzymes in response to temperature: a cross‐latitudinal study, Global Change Biology, 18, 1468-1479, 2012.

Hicke, J. A. and Lobell, D. B.: Spatiotemporal patterns of cropland area and net primary production in the central United States estimated from USDA agricultural information, Geophysical Research Letters, 31, 2004.

Mayes, M. A., Heal, K. R., Brandt, C. C., Phillips, J. R., and Jardine, P. M.: Relation between Soil Order and Sorption of Dissolved Organic Carbon in Temperate Subsoils, Soil Science Society of America Journal, 76, 1027-1037, 10.2136/sssaj2011.0340, 2012.

Parton, W. J., Morgan, J. A., Kelly, R. H., and Ojima, D.: Modeling soil C responses to environmental change in grassland systems[M] The potential of US grazing lands to sequester carbon and mitigate the greenhouse effect, 2000.

Wang, G., Huang, W., Zhou, G., Mayes, M. A., and Zhou, J.: Modeling the processes of soil moisture in regulating microbial and carbon-nitrogen cycling, Journal of Hydrology, 585, 10.1016/j.jhydrol.2020.124777, 2020.

Wang, J., Xiong, Z., and Kuzyakov, Y.: Biochar stability in soil: meta-analysis of decomposition and priming effects, Global Change Biology Bioenergy, 8, 512-523, 10.1111/gcbb.12266, 2016.

Wieder, W. R., Grandy, A. S., Kallenbach, C. M., and Bonan, G. B.: Integrating microbial physiology and physio-chemical principles in soils with the MIcrobial-MIneral Carbon Stabilization (MIMICS) model, Biogeosciences, 11, 3899-3917, 10.5194/bg-11-3899-2014, 2014.

Wieder, W. R., Grandy, A. S., Kallenbach, C. M., Taylor, P. G., and Bonan, G. B.: Representing life in the Earth system with soil microbial functional traits in the MIMICS model, Geoscientific Model Development, 8, 1789-1808, 10.5194/gmd-8-1789-2015, 2015.

Yan, Z., Bond-Lamberty, B., Todd-Brown, K. E., Bailey, V. L., Li, S., Liu, C., and Liu, C.: A moisture function of soil heterotrophic respiration that incorporates microscale processes, Nat Commun, 9, 2562, 10.1038/s41467-018-04971-6, 2018.

Zhang, H., Goll, D. S., Wang, Y. P., Ciais, P., Wieder, W. R., Abramoff, R., Huang, Y., Guenet, B., Prescher, A. K., Viscarra Rossel, R. A., Barre, P., Chenu, C., Zhou, G., and Tang, X.: Microbial dynamics and soil physicochemical properties explain large-scale variations in soil organic carbon, Glob Chang Biol, 10.1111/gcb.14994, 2020.